ISSN 1990-7931, Russian Journal of Physical Chemistry B, 2015, Vol. 9, No. 2, pp. 172–184. © Pleiades Publishing, Ltd., 2015.
Original Russian Text © G.S. Borodkin, Yu.E. Chernysh, V.A. Volynkin, V.T. Panyushkin, 2015, published in Khimicheskaya Fizika, 2015, Vol. 34, No. 4, pp. 6–19.

## STRUCTURE OF CHEMICAL COMPOUNDS. SPECTROSCOPY

# Application of Selective Two-Dimensional Exchange NMR Spectroscopy to the Study of Molecular Dynamic Processes

**G. S. Borodkin[a], Yu. E. Chernysh[a], V. A. Volynkin[b], and V. T. Panyushkin[b]**

[a] *Institute of Physical and Organic Chemistry, Southern Federal University, pr. Stachki 194/2, Rostov-on-Don, 344090 Russia*

[b] *Kuban State University, Stavropol'skaya ul. 149, Krasnodar, 360040 Russia*

*e-mail: yu.chern@rambler.ru*

Received October 30, 2013

**Abstract**—A vector model of the multiplet-selective excitation of spin systems by a three-pulse sequence is considered, and, on this basis, a new two-dimensional exchange NMR spectroscopy technique is suggested. This technique provides means to investigate intramolecular and intermolecular chemical and spin exchanges by observing the dynamic behavior of the multiplet pattern of a nucleus that is scalarwise coupled with the unobservable nucleus undergoing exchange.

*Keywords*: molecular structure, exchange spectroscopy, multiplet-selective excitation

**DOI:** 10.1134/S1990793115020190

## INTRODUCTION

At present, there are numerous selective experimental NMR techniques intended for the study of molecular behaviors in the liquid and solid states [1–4]. Here, we present a new technique for investigating molecular dynamic processes. In this technique, only one nucleus of a coupled spin system is excited.

Earlier, we described a procedure in which coherent transfer effects are suppressed by the multiplet-selective excitation (MUSEX) of the spin system [5]. The usefulness of this technique lies in the fact that it minimizes the loss of information about spin–spin coupling. Its drawback is that information on the chain of scalarwise coupled spins is lost in the study of exchange processes. In order to avoid this situation, it is necessary to combine selective and nonselective excitations in the NMR experiment.

Three-pulse sequences are used in the experiment suggested here. Each sequence is a combination of two multiplet-selective pulses and one nonselective pulse. The MUSEX EXSY experiment is a combination of correlation spectroscopy (COSY) methods and exchange spectroscopy (EXSY) methods. We will consider all possible combinations of nonselective and selective pulses. There are altogether 32 variants of the experiment, and an appropriate pulse sequence should be selected for solving a particular problem. All our calculations are based on the vector operator formalism (VOF) [6]. The results will be presented for sequences exciting the weakly coupled system AX (IS). The main distinctive feature of these sequences is use of alternating excitation (ALEX) of spins based on multiplet-selective excitation (MUSEX).

## MUSEX EXSY EXPERIMENT

### *Vector Operator Formalism*

Here, we will discuss the results obtained by applying the vector operator formalism [7] to a system of two coupled spins (IS = AX) subjected to the action of the pulse sequences specified below.

**I. Pulse sequence $[90^\circ_x - t_1 - 90^\circ_x(\mathrm{I}) - \tau_{mix} - 90^\circ_x(\mathrm{I}) - t_2]_n$.** Note that the first pair of pulses in this sequence is actually a MUSEX COSY experiment [8]. After the action of the second selective pulse exciting nucleus I, the remaining transverse components continue to precess at the same frequency as within the period $t_1$ and the longitudinal components are involved in exchange processes (if the latter take place) during the mixing period $\tau_{mix}$. The third, selective, 90° pulse, applied to the nucleus A, serves to record the signal.

The third, $90^\circ_x(\mathrm{I})$ pulse about the $x$ axis leaves only the $x$-components . Only nucleus I is re-excited here. This means that the spectrum for the nucleus I is unchanged, as was demonstrated for the case of two selective pulses applied to the nucleus I (see the table in [6]). As for the nucleus S, since the channels for S are closed, the resonance lines of the square multiplet pattern that lie precisely on the diagonal disappear, while the nondiagonal lines remain, as is proved by calculations based on the formalism suggested here (see below). The spin diagram for the nucleus I is shown in Fig. 1. Trigonometric transformations eventually yield the same positions of the signals from the

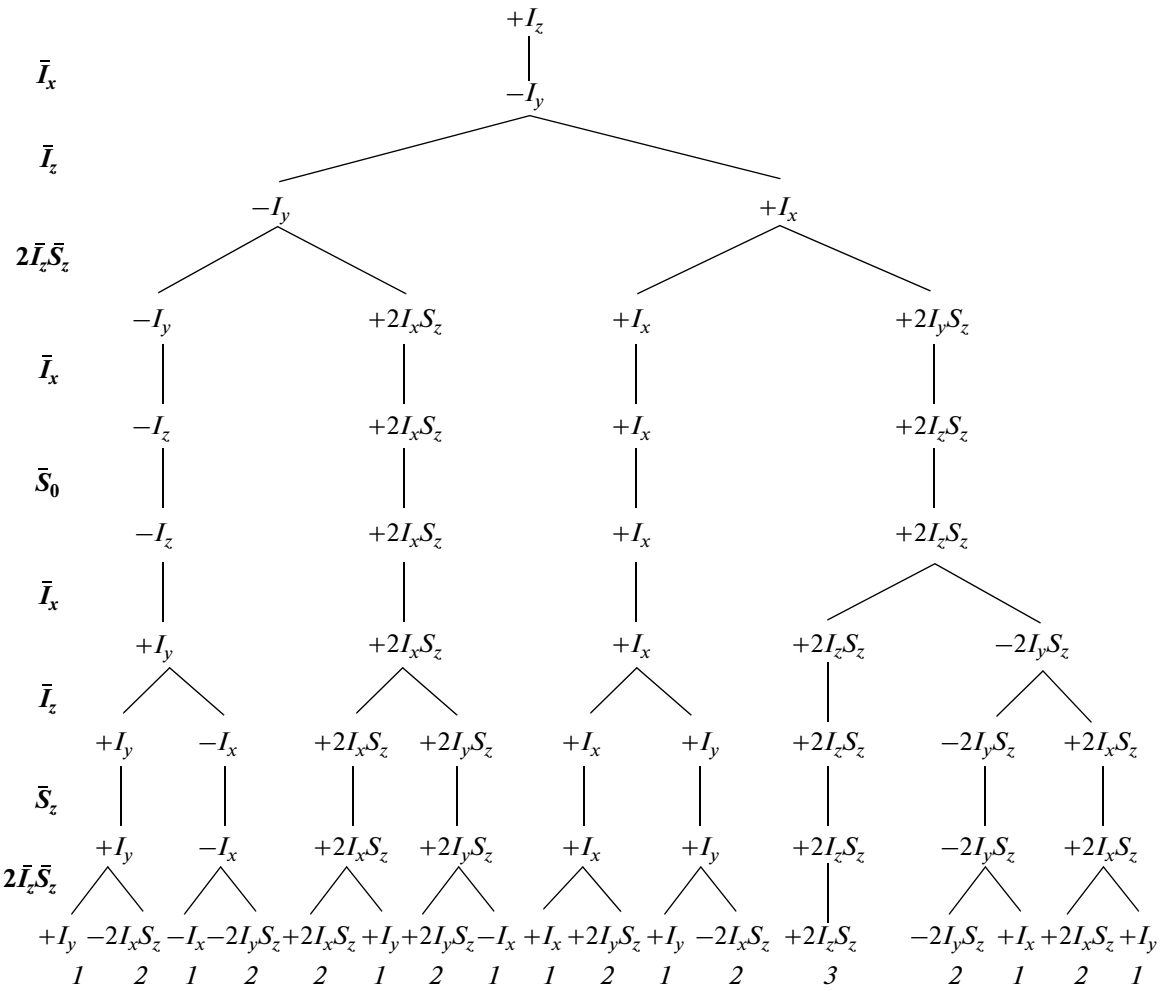


**Fig. 1.** Diagram of the evolution of the vector operators of spin I in the COSY experiment: (*1*) diagonal peaks, (*2*) antiphase magnetization, and (*3*) longitudinal magnetization.

spin of I as in the case of the two-pulse sequence $[90^\circ_x - t_1 - 90^\circ_x(\mathrm{I}) - t_2]$.

For the spin of S, the four pathways that lead to the observable *y*-components appear in complete form as follows:

$$\sigma_4^1 = -S_y\cos\omega_S t_1\cos\pi J_{IS}t_1\cos\omega_S t_2\cos\pi J_{IS}t_2$$
$$= -\frac{1}{4}S_y[\cos(\omega_S - \pi J_{IS})t_1 + \cos(\omega_S + \pi J_{IS})t_1]$$
$$\times [\cos(\omega_S - \pi J_{IS})t_2 + \cos(\omega_S + \pi J_{IS})t_2]$$
$$= -\frac{1}{4}S_y[\cos(\omega_S - \pi J_{IS})t_1\cos(\omega_S - \pi J_{IS})t_2 + \cos(\omega_S$$
$$- \pi J_{IS})t_1\cos(\omega_S + \pi J_{IS})t_2 + \cos(\omega_S + \pi J_{IS})t_1\cos(\omega_S$$
$$- \pi J_{IS})t_2 + \cos(\omega_S + \pi J_{IS})t_1\cos(\omega_S + \pi J_{IS})t_2],$$

$$\sigma_4^2 = -S_y\cos\omega_S t_1\sin\pi J_{IS}t_1\cos\omega_S t_2\sin\pi J_{IS}t_2 = -\frac{1}{4}S_y$$
$$\times [\sin(\omega_S + \pi J_{IS})t_1 - \sin(\omega_S - \pi J_{IS})t_1][\sin(\omega_S + \pi J_{IS})$$
$$t_2 - \sin(\omega_S - \pi J_{IS})t_2] = -\frac{1}{4}S_y[\sin(\omega_S + \pi J_{IS})\ t_1$$
$$\times \sin(\omega_S + \pi J_{IS})t_2 - \sin(\omega_S + \pi J_{IS})t_1\sin(\omega_S - \pi J_{IS})t_2$$
$$- \sin(\omega_S - \pi J_{IS})t_1\sin(\omega_S + \pi J_{IS})t_2 + \sin(\omega_S - \pi J_{IS})$$
$$\times t_1\sin(\omega_S - \pi J_{IS})t_2],$$

$$\sigma_4^3 = S_y\sin\omega_S t_1\cos\pi J_{IS}t_1\sin\omega_S t_2\cos\pi J_{IS}t_2 = \frac{1}{4}S_y$$
$$\times [\sin(\omega_S - \pi J_{IS})t_1 + \sin(\omega_S + \pi J_{IS})t_1][\sin(\omega_S - \pi J_{IS})$$
$$\times t_2 + \sin(\omega_S + \pi J_{IS})t_2] = \frac{1}{4}S_y[\sin(\omega_S - \pi J_{IS})t_1$$
$$\times \sin(\omega_S - \pi J_{IS})t_2 + \sin(\omega_S - \pi J_{IS})t_1\sin(\omega_S + \pi J_{IS})t_2$$
$$+ \sin(\omega_S + \pi J_{IS})t_1\sin(\omega_S - \pi J_{IS})t_2 + \sin(\omega_S + \pi J_{IS})$$
$$\times t_1\sin(\omega_S + \pi J_{IS})t_2],$$

$$\sigma_4^4 = S_y\sin\omega_S t_1\sin\pi J_{IS}t_1\sin\omega_S t_2\sin\pi J_{IS}t_2 = \frac{1}{4}S_y$$
$$\times [\cos(\omega_S - \pi J_{IS})t_1 - \cos(\omega_S + \pi J_{IS})t_1][\cos(\omega_S$$
$$- \pi J_{IS})t_2 - \cos(\omega_S + \pi J_{IS})t_2] = \frac{1}{4}S_y[\cos(\omega_S - \pi J_{IS})$$
$$\times t_1\cos(\omega_S - \pi J_{IS})t_2 - \cos(\omega_S - \pi J_{IS})t_1\cos(\omega_S + \pi J_{IS})t_2$$

**Table 1.** $y$-Components of the density operator in the $t_2$ step, represented as 2D spectra for two coupled nuclei

| Nucleus A | Diagonal peaks | Nucleus B | Diagonal peaks |
|---|---|---|---|
| $I_{Ay}C_{A_1}C_{AB_1}C_{A_2}C_{AB_2}$ | ● ●<br>● ● | $-I_{By}C_{B_1}C_{AB_1}C_{Am}C_{ABm}C_{B_2}C_{AB_2}$ | ○ ○<br>○ ○ |
| $I_{Ay}C_{A_1}S_{AB_1}C_{Am}C_{ABm}C_{A_2}S_{AB_2}$ | ○ ●<br>● ○ | $-I_{By}C_{B_1}S_{AB_1}C_{Am}C_{ABm}C_{B_2}S_{AB_2}$ | ● ○<br>○ ● |
| $I_{Ay}S_{A_1}C_{AB_1}C_{Am}C_{ABm}C_{A_2}C_{AB_2}$ | ● ●<br>● ● | $I_{By}S_{B_1}C_{AB_1}C_{Am}C_{ABm}C_{B_2}C_{AB_2}$ | ● ●<br>● ● |
| $I_{Ay}S_{A_1}S_{AB_1}S_{A_2}S_{AB_2}$ | ● ○<br>○ ● | $I_{By}S_{B_1}S_{AB_1}C_{Am}C_{ABm}S_{B_2}S_{AB_2}$ | ○ ●<br>● ○ |
| $-I_{Ay}C_{A_1}S_{AB_1}S_{Am}S_{ABm}S_{A_2}C_{AB_2}$ | ● ○<br>● ○ | $I_{By}C_{B_1}C_{AB_1}S_{Am}C_{ABm}S_{B_2}C_{AB_2}$ | ● ●<br>● ● |
| $-I_{Ay}S_{A_1}C_{AB_1}S_{Am}S_{ABm}C_{A_2}S_{AB_2}$ | ○ ○<br>● ● | $I_{By}C_{B_1}S_{AB_1}C_{Am}S_{ABm}S_{B_2}S_{AB_2}$ | ● ○<br>○ ● |
| | | $I_{By}S_{B_1}C_{AB_1}S_{Am}C_{ABm}C_{B_2}C_{AB_2}$ | ● ●<br>● ● |
| | | $I_{By}S_{B_1}S_{AB_1}C_{Am}S_{ABm}C_{B_2}S_{AB_2}$ | ● ○<br>○ ● |

$C_{A_{1(2)}(B_{1(2)})} = \cos\Omega_{A(B)}t_{1(2)}$; $C_{A(B)m} = \cos\Omega_{A(B)}t_m$; $C_{AB_{1(2)}} = \cos\pi J_{AB}t_{1(2)}$; $C_{A(B)m} = \cos\pi J_{AB}t_m$; $S_{A_{1(2)}(B_{1(2)})} = \sin\Omega_{A(B)}t_{1(2)}$; $S_{A(B)m} = \sin\Omega_{A(B)}t_m$; $S_{AB_{1(2)}} = \sin\pi J_{AB}t_{1(2)}$; $S_{A(B)m} = \sin\pi J_{AB}t_m$; $I_{A(B)y}$ is in-phase magnetization; ●, positive intensity of the absorption signal; ○, negative intensity of the absorption signal.

$$- \cos(\omega_S + \pi J_{IS})t_1\cos(\omega_S - \pi J_{IS})t_2$$
$$+ \cos(\omega_S + \pi J_{IS})t_1\cos(\omega_S + \pi J_{IS})t_2].$$

By summing these expressions and grouping like terms, we obtain

$$\sigma_4^{obs} = -\frac{1}{2}S_y[\cos(\omega_S - \pi J_{IS})t_1\cos(\omega_S + \pi J_{IS})t_2$$
$$+ \cos(\omega_S + \pi J_{IS})t_1\cos(\omega_S - \pi J_{IS})t_2] + \frac{1}{2}S_y[\sin(\omega_S + \pi J_{IS})$$
$$\times t_1\sin(\omega_S - \pi J_{IS})t_2 + \sin(\omega_S - \pi J_{IS})t_1\sin(\omega_S + \pi J_{IS})t_2].$$

For comparison, we list, in Table 1, the observable terms of the density operator that describe the behavior of the system of two coupled spins during the precession period $t_2$. In Table 2, we schematize some of the calculated spectra for three-pulse sequences. As is clear from Table 2, the cross peak pattern for these sequences is significantly simplified, depending on the mixing coefficient.

The spectrum is of use in the study of exchange processes occurring in complex spin systems, particularly in systems characterized by overlapping and overcrowded regions. Therefore, this method can be used to prove the existence of a dynamic process in molecular systems. Exchange processes can also be observed using the diagonal and cross peak model. After the excitation of any random exchange processes, resonance exchange lines appear inside diagonal peaks; in other words, the square pattern of these peaks is restored.

**II. Pulse sequence $[90^\circ_x(A) - t_1 - 90^\circ_x - \tau_{mix} - 90^\circ_x(A) - t_2]_n$.** The observable terms of the AX system can be represented in the same way as in the previous case. The two-dimensional (2D) spectrum is actually one of the two symmetric halves of the standard spectrum. In the 2D spectrum, the signal from the S (A) nuclei is unobservable:

$$\sigma = -S_y\cos\omega_S t_2\cos\pi J t_2$$
$$= -\frac{1}{2}[S_y(\cos(\omega_S - \pi J)t_2 + \cos(\omega_S + \pi J)t_2)].$$

**III. Pulse sequence $[90^\circ_x(A) - t_1 - 90^\circ_x(A) - \tau_{mix} - 90^\circ_x - t_2]_n$.** As would be expected, the spectrum in this case degenerates again, changing its cross peak pattern relative to that in the two previous cases. Note that the two selective pulses in the alternating excitation (ALEX) of the A/X nuclei (one 90° (A/X) pulse and

**Table 2.** Variants of the MUSEX EXSY experiment

| Technique | Pulse sequence | 2D spectra |
|---|---|---|
| NSP-NSP-SP(A) | $[90^\circ_x - t_1 - 90^\circ_x - \tau_{mix} - 90^\circ_x(A) - t_2]_n$ | 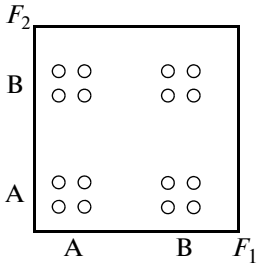 |
| NSP-SP(A)-NSP | $[90^\circ_x - t_1 - 90^\circ_x(A) - \tau_{mix} - 90^\circ_x - t_2]_n$ | 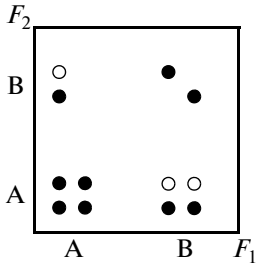 |
| SP(A)-NSP-NSP | $[90^\circ_x(A) - t_1 - 90^\circ_x - \tau_{mix} - 90^\circ_x - t_2]_n$ | 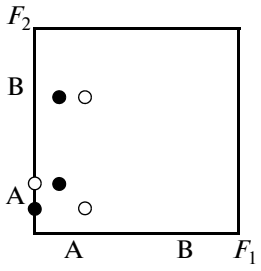 |
| NSP-SP(A)-SP(A) | $[90^\circ_x - t_1 - 90^\circ_x(A) - \tau_{mix} - 90^\circ_x(A) - t_2]_n$ | 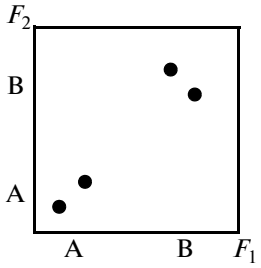 |
| SP(A)-NSP-SP(A) | $[90^\circ_x(A) - t_1 - 90^\circ_x - \tau_{mix} - 90^\circ_x(A) - t_2]_n$ | 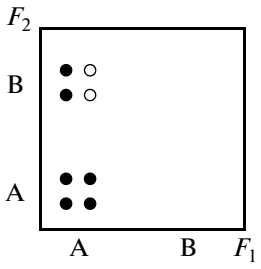 |

**Table 2.** (Contd.)

| Technique | Pulse sequence | 2D spectra |
|---|---|---|
| SP(A)-SP(A)-NSP | $[90^\circ_x(\mathrm{A}) - t_1 - 90^\circ_x(\mathrm{A}) - \tau_{mix} - 90^\circ_x - t_2]_n$ | 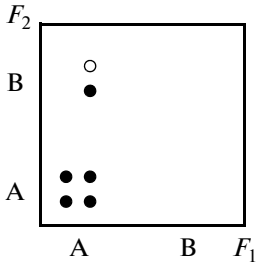  |
| SP(A)-SP(A)-SP(B) | $[90^\circ_x(\mathrm{A}) - t_1 - 90^\circ_x(\mathrm{A}) - \tau_{mix} - 90^\circ_x(\mathrm{B}) - t_2]_n$ | 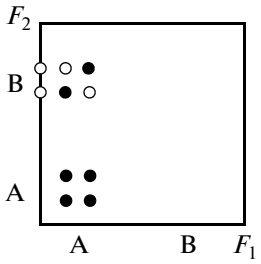  |
| SP(A)-SP(B)-SP(A) | $[90^\circ_x(\mathrm{A}) - t_1 - 90^\circ_x(\mathrm{B}) - \tau_{mix} - 90^\circ_x(\mathrm{A}) - t_2]_n$ | 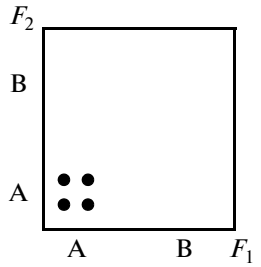  |
| SP(B)-SP(A)-SP(A) | $[90^\circ_x(\mathrm{B}) - t_1 - 90^\circ_x(\mathrm{A}) - \tau_{mix} - 90^\circ_x(\mathrm{A}) - t_2]_n$ | 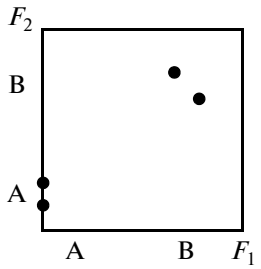  |

one 90° (X/A) pulse) give reflection-symmetric 2D spectra (Fig. 2).

Sequences I and III provide means to visualize each coupling in a multiplet system and chemical exchange. Thus, these sequences can be used step-by-step to identify all coupled partners in a complex spin system, since the above-considered MUSEX COSY experiment makes it possible to observe all couplings simultaneously. Sequence I is convenient in the investigation of relaxation mechanisms. The resulting spectrum in the case of sequence II has a diagonal peak from the spin of A as a consequence of the interference of eight components, among which four ones arise from single-quantum coherences and the others arise from two-quantum and zero-quantum coherences. In this case, the first two pulses are ALEX COSY and the third pulse, applied to the nucleus X, is used as the detecting pulse. As $\tau_{mix}$ is varied, the two rectangular lines for the diagonal peaks may disappear, leaving the diagonal lines.

Note that the set of these sequences can be considered as a complete MUSEX EXSY experiment. This experiment has the following advantages over standard EXSY spectroscopy:

(1) Assignment of resonance signals in a complicated NMR spectrum is easier to do and is more unambiguous.

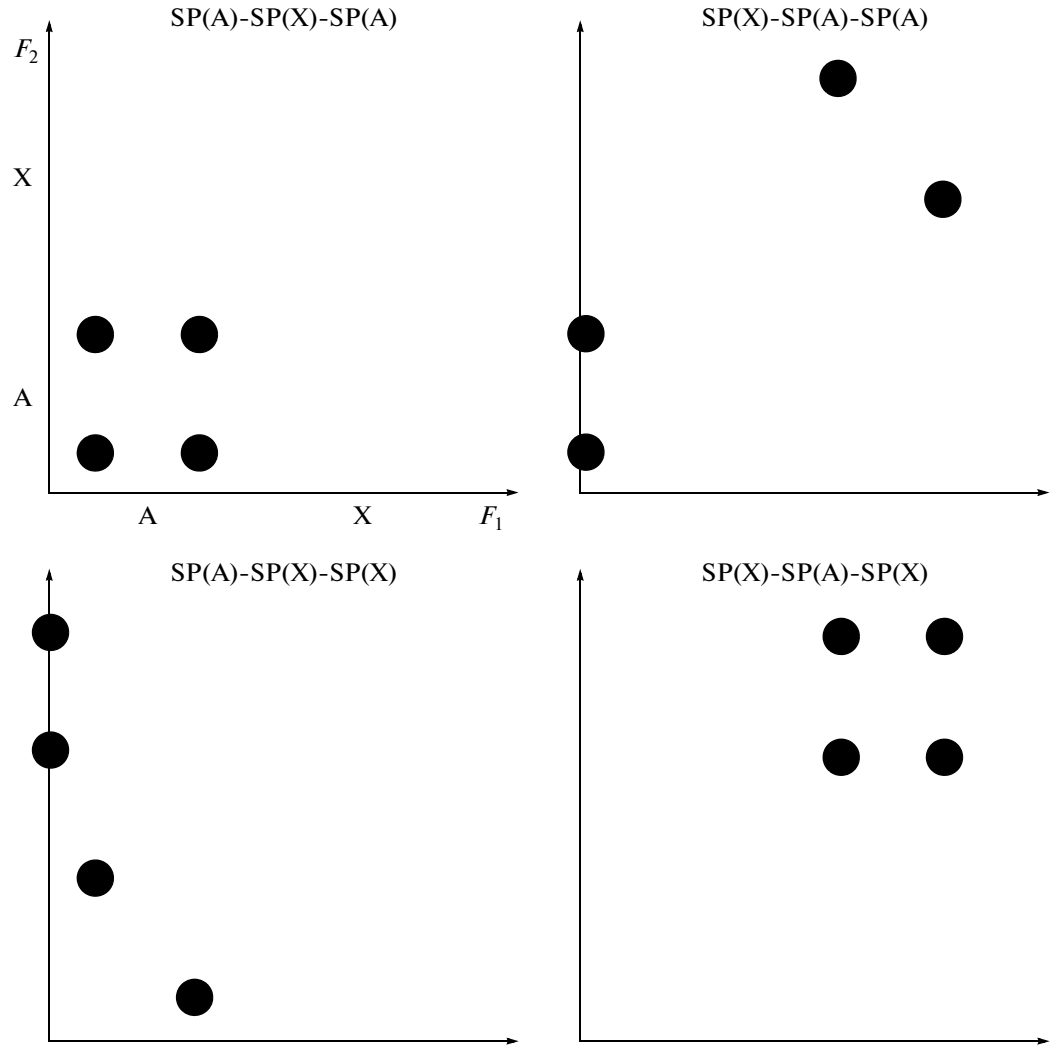


**Fig. 2.** Variants of the ALEX EXSY experiment. SP(A)/(X) is the selective pulse.

(2) This method can readily be carried out in practice, since any spectrometer fitted with a selective attachment is suitable for its implementation.

(3) This method is particularly helpful in proving the uniqueness of an exchange mechanism.

(4) Selective pulses are used in this experiment.

In addition, the above calculations coincide with the classical description and, as will be demonstrated below, with strict quantum chemical calculations [9].

### *Quantum Chemical Interpretation of the Method*

Consider the pulse sequence $[90^\circ_x - t_1 - 90^\circ_x(\mathrm{A}) - \tau_{mix} - 90^\circ_x(\mathrm{A}) - t_2]_n$ exciting the spin system AX. The transformation matrix of the rotation operator $((1/2)R_x(\pi/2))$ in explicit form in the orthonormal basis appears as follows [10, 11]:

$$\begin{pmatrix} 1 & i & i & -1 \\ i & 1 & -1 & i \\ i & -1 & 1 & i \\ -1 & i & i & 1 \end{pmatrix}.$$

The density matrix for a thermally equilibrated system appears as

$$\sigma_{eq} = \frac{1}{4}\begin{pmatrix} 1+p & 0 & 0 & 0 \\ 0 & 1 & 0 & 0 \\ 0 & 0 & 1 & 0 \\ 0 & 0 & 0 & 1-p \end{pmatrix} = \frac{1}{4}\mathrm{E} + \frac{p}{4}\begin{pmatrix} 1 & 0 & 0 & 0 \\ 0 & 0 & 0 & 0 \\ 0 & 0 & 0 & 0 \\ 0 & 0 & 0 & -1 \end{pmatrix},$$

where $\sigma_{eq} = \sigma_0$ ($\sigma_0$ is the density matrix at $t = 0$), $p = \hbar\omega_A/kT$, $\omega_A$ is the Larmor frequency of the spin of A; $\omega_A = \omega_X$, since populations are considered. In the calculations presented below, it is possible to omit the first term, since the rotation operator $R_x$ commutes

with the unit operator. We will then obtain $\sigma_1 = R_x^{-1}(\pi/2)\sigma_0 R_x(\pi/2)$ or, in matrix notation,

$$\sigma_1 = -\frac{ip}{8}\begin{pmatrix} 0 & -1 & -1 & 0 \\ 1 & 0 & 0 & -1 \\ 1 & 0 & 0 & -1 \\ 0 & 1 & 1 & 0 \end{pmatrix}.$$

In the evolution period $t_1$, the system being irradiated evolves under the action of precession in the following way:

$$\sigma_2 = \frac{ip}{16}\begin{pmatrix} 0 & -e_{12} & -e_{13} & 0 \\ e_{21} & 0 & 0 & -e_{24} \\ e_{31} & 0 & 0 & -e_{34} \\ 0 & e_{42} & e_{43} & 0 \end{pmatrix},$$

where $e_{nm}$ designates the $\exp(i\omega_{nm}t_1)$ exponentials, $\omega_{13} = \omega_{A_1} = \omega_A - \pi J$, $\omega_{12} = \omega_{X_1} = \omega_X - \pi J$, $\omega_{24} = \omega_{A_2} = \omega_A + \pi J$, and $\omega_{34} = \omega_{X_2} = \omega_X + \pi J$.

The second pulse, which is selective toward the nucleus A, $(\pi/2)_x(A)$, generates the following state: $\sigma_3 = R_x^{-1}(\pi/2)_A\sigma_2 \times R_x(\pi/2)_A$, or

$$\frac{ip}{16}\begin{pmatrix} -i(e_{13}+e_{31}) & -(e_{12}+e_{34}) & (-e_{13}+e_{31}) & i(-e_{12}+e_{34}) \\ (e_{21}+e_{43}) & -i(e_{24}+e_{42}) & i(e_{21}-e_{43}) & (-e_{24}+e_{42}) \\ (-e_{13}+e_{31}) & i(e_{12}-e_{34}) & i(e_{13}+e_{31}) & -(e_{12}+e_{34}) \\ i(-e_{21}+e_{43}) & (-e_{24}+e_{42}) & (e_{21}+e_{43}) & i(e_{24}+e_{42}) \end{pmatrix}.$$

Since $\exp(i\omega_{31}t_1) = \exp(-i\omega_{13}t_1)$, $\exp(i\omega_{42}t_1) = \exp(-i\omega_{24}t_1)$, and so on, introducing the designations $\sin\omega_{13}t_1 = S_{A_1}$, $\sin\omega_{24}t_1 = S_{A_2}$, $\cos\omega_{13}t_1 = C_{A_1}$, and $\cos\omega_{24}t_1 = C_{A_2}$, we obtain

$$\sigma_{3p} = \frac{p}{8}\begin{pmatrix} 1-C_{A_1} & 0 & 0 & 0 \\ 0 & -1-C_{A_2} & 0 & 0 \\ 0 & 0 & 1+C_{A_1} & 0 \\ 0 & 0 & 0 & -1+C_{A_2} \end{pmatrix},$$

$$\sigma_{3s} = \frac{p}{8}\begin{pmatrix} 0 & \begin{Bmatrix} -iC_{X_1}+S_{X_1}- \\ -iC_{X_2}+S_{X_2} \end{Bmatrix} & S_{A_1} & 0 \\ \begin{Bmatrix} iC_{X_1}-S_{X_1}+ \\ +iC_{X_2}-S_{X_2} \end{Bmatrix} & 0 & 0 & S_{A_2} \\ S_{A_1} & 0 & 0 & \begin{Bmatrix} -iC_{X_1}+S_{X_1}- \\ -iC_{X_2}+S_{X_2} \end{Bmatrix} \\ 0 & S_{A_2} & \begin{Bmatrix} iC_{X_1}+S_{X_1}+ \\ +iC_{X_2}+S_{X_2} \end{Bmatrix} & 0 \end{pmatrix},$$

where the component $\sigma_{3p}$ represents populations and consists of two parts, one of them being the population tagged with the frequencies of the excited transitions. The single-quantum coherence $\sigma_{3s}$ is responsible for the observed transverse magnetization of the spins of A and X. Obviously, no coherence transfer is observed for the spin of A. As for the spin of X, the $1 \to 2$ transition between the energy levels of the AX spin system turns out to be modulated by both frequencies of the spin of X, namely $C_{X_1} + iS_{X_1}$ and $C_{X_2} + iS_{X_2}$. This means that, during the evolution period $t_2$, the $1 \to 2$ transition, tagged with the spin $X_1$ frequency, leads to the mixing of the frequencies of the spins of $X_1$ and $X_2$; that is, after a double Fourier transform, peaks at the frequencies $(F_{X_1}, F_{X_1})$ and $(F_{X_2}, F_{X_1})$ appear in the 2D spectrum. By similar considerations for the $2 \to 4$ transition, we obtain two more peaks, namely, $(F_{X_1}, F_{X_2})$ and $(F_{X_2}, F_{X_2})$.

It is of interest to consider the 2D spectrum that results from the action of the second selective pulse $\pi_x(A)$, in place of the $(\pi/2)_x(A)$ pulse, on the AX system. Now the second selective pulse, applied to the nucleus A, generates the following state: $\sigma_3 = R_x^{-1}(\pi)_A\sigma_2 R_x(\pi)_A$ or, in matrix notation,

$$\frac{ip}{4}\begin{pmatrix} 0 & -e_{34} & e_{31} & 0 \\ e_{43} & 0 & 0 & e_{42} \\ -e_{13} & 0 & 0 & -e_{12} \\ 0 & -e_{24} & e_{21} & 0 \end{pmatrix}.$$

After a double Fourier transform, we obtain a unique 2D spectrum in which there are no strictly diagonal peaks due to the nucleus X. Obviously, this 2D spectral pattern makes it possible to unambiguously determine scalar couplings for two coupled spins in an analysis of NMR spectra, particularly for macromolecules.

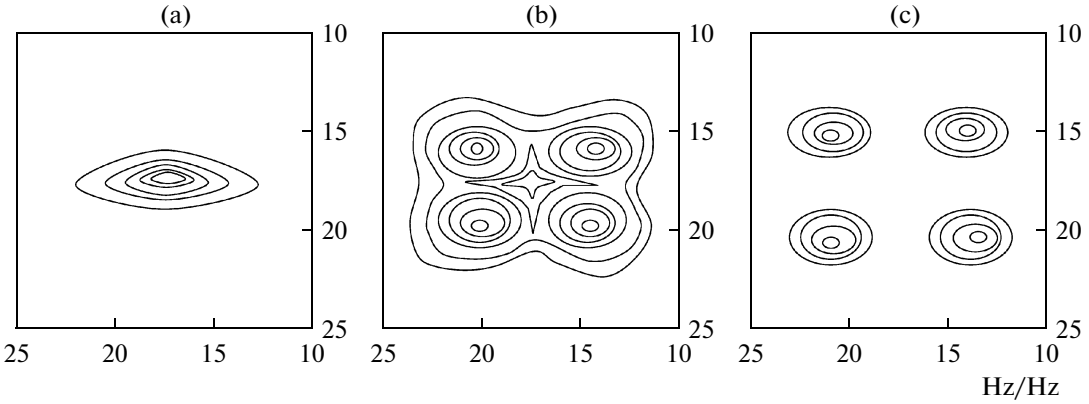


**Fig. 3.** Nonselective 2D exchange proton NMR spectra of methanol recorded in the $CH_3$ group region ($f = 100$ MHz) at (a) 22, (b) −42, and (c) −70°C.

Returning to the three-pulse sequence $[90^\circ_x - t_1 - 90^\circ_x(\mathrm{A}) - \tau_{mix} - 90^\circ_x(\mathrm{A}) - t_2]_n$, we can draw the conclusion that the two selective pulses exciting the nucleus A act on the AX spin system in the same way as the single selective pulse $\pi_x(\mathrm{A})$ does. The ultimate effect of this pulse sequence differs from the effect of the pulse sequence $[90^\circ_x - t_1 - 180^\circ_x(\mathrm{A})]_n$ by the coefficient $e_{ij}(\tau_{mix})$ and the signals from the nucleus X that lie strictly on the diagonal disappear from the spectrum. If the spin system undergoes exchange processes, then the square pattern of the diagonal peaks from both nuclei will restore and exchange cross peaks will appear.

## RESULTS AND DISCUSSION

To achieve the purpose of the experiment, NMR spectra were recorded on Varian and Bruker spectrometers operating at 100, 200, 300, and 500 MHz. The solvents were chloroform-$d_1$, acetone-$d_6$, water-$d_2$, methylene chloride, dimethyl sulfoxides-$d_6$, nitrobenzene-$d_5$, bromobenzene-$d_5$, and toluene-$d_8$. Prior to being used in an experiment, the solvents were held over molecular sieve 4 Å for at least 1 day.

The kinetics of the observed dynamic processes was quantitatively studied by recording the temperature evolution of line shape of indicator signals in NMR spectra and by comparing the experimental spectra with the set of theoretically calculated lifetimes of exchanging states ($\tau_c$, s) [7].

The two types of spectra were matched by comparing their characteristic parameters, namely, the full width at half-maximum of the lines, interpeak distance, the ratio of the maximum signal amplitude to central minimum, etc.

### *Methanol*

The advantages of the MUSEX technique will be demonstrated using intermolecular proton exchange in methanol as an example [7]. The one-dimensional $^1$H NMR spectrum of methanol in the absence of chemical exchange is well known. The fine structure of the spectrum shows itself because the chemical exchange in methanol slows down as the sample temperature is decreased.

This chemical exchange in methanol is known to proceed via the following reaction:

$$\mathrm{CH_3^{(1)}OH^{(1)} + CH_3^{(2)}OH^{(2)}} \leftrightarrow \mathrm{CH_3^{(1)}OH^{(2)} + CH_3^{(2)}OH^{(1)}}. \quad (1)$$

Investigation of process (1) in the temperature range from −70 to 40°C by means of conventional 2D exchange spectroscopy using a standard three-pulse sequence without suppressing all types of coherences seems to be impossible, because the nonselective multiple-pulse excitation of the coupled spin system of $CH_3OH$ causes coherent magnetization transfer along the scalar coupling chains ($J$ cross peaks). Therefore, the exchange cross peaks will overlap with $J$ cross peaks and information concerning chemical exchange will be lost. Indeed, in the case of nonselective excitation (Fig. 3), the intramultiplet cross peaks (ICPs) observed at −42°C might seem to be evidence of an exchange process taking place owing to the averaging of the indirect spin–spin coupling constant $^3J_{HH}$ as a result of intramolecular proton exchange between hydroxyl groups. However, as this exchange is further frozen (the temperature is lowered to −70°C), the ICPs in the spectrum persist, and this can only be due to coherent magnetization transfer in the coupled spin system, which is nonselectively excited in this case.

The MUSEX excitation of either proton-containing group of methanol causes no coherent magnetization transfer between the coupled transitions, as was demonstrated above. This is the reason why the signal from the methyl group, at −70°C, when there is no

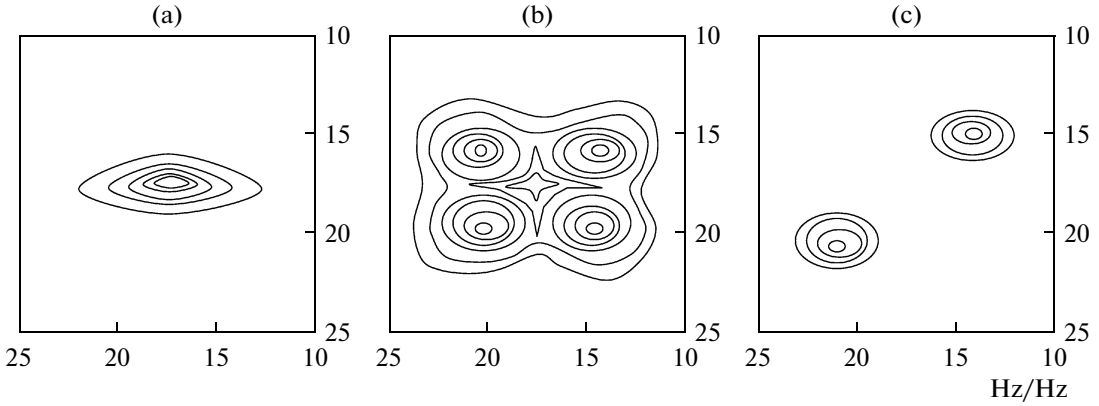


**Fig. 4.** MUSEX 2D exchange proton NMR spectra of methanol recorded in the $CH_3$ group region at (a) 22, (b) –42, and (c) –70°C.

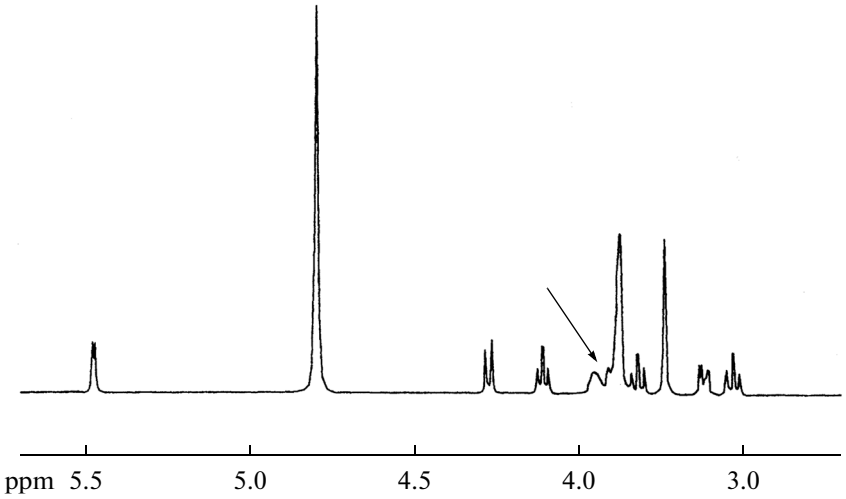


**Fig. 5.** One-dimensional $^1$H NMR spectrum of sucrose (500 MHz). The arrow indicates the signal from H(5').

chemical exchange (reaction (1)), as distinct from the same signal shown in Fig. 3, consists of only two resonance lines located along the principal diagonal of the 2D exchange spectrum (Fig. 4). Likewise, the four resonance lines of the signal from the hydroxyl proton are observed. Once the chemical exchange begins, ICPs appear in the spectrum and the intensity of these peaks increases as the rate of exchange is increased by raising the sample temperature. Thus, the MUSEX 2D exchange spectra obtained describe only pure chemical exchange in methanol.

The advantage of pulse sequence II in the assignment of chemical shifts of resonance signals will be demonstrated using the NMR spectrum of sucrose as an example.

It is very often impossible to selectively excite the proton signal if the latter is in a heavily overlapped spectral range or in the immediate vicinity of other signals, as in the case of the H(5') proton in the 500 MHz $^1$H NMR spectrum of sucrose in $D_2O$ (Fig. 5).

Nevertheless, in a proton magnetic resonance spectrum of any complexity, there is always a well-resolved resonance line that can be selectively excited with a high spectral purity (e.g., the proton H(1') line) by using one of the above pulse sequences, such as $[90^\circ_x(\mathrm{H}-1') - t_1 - 90^\circ_x - t_2]_n$. The first, selective pulse excites only the H(1') proton, which is registered at some frequency during the time period $t_1$. The second, nonselective, mixing pulse serves to transfer the frequency-registered coherent magnetization of the H(1') proton only to the protons that are scalarwise coupled with it. Figure 6 shows its 2D spectrum. The first, selective pulse excites the H(1') proton. The spectrum displays only the signal from the H(2') proton, which is scalarwise coupled with H(1').

### *Mechanism of Degenerate Ligand Exchange Reactions in Cadmium Complexes*

The scientific literature contains many examples of how a change in spin–spin splitting is used to carry out

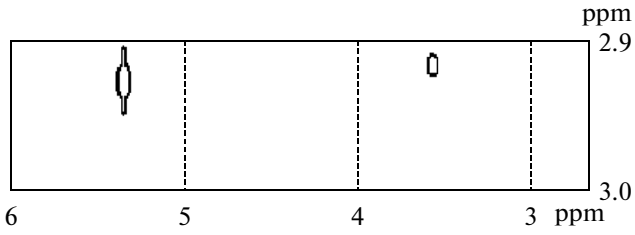


**Fig. 6.** Two-dimensional $^1$H NMR spectrum of sucrose (500 MHz).

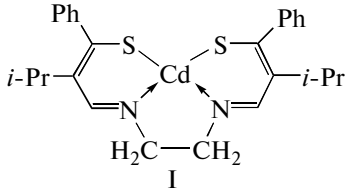


I

**Fig. 7.** Structural formula of *N*,*N*'-ethylenebis(α-isopropyl-β-mercaptopropylenealdiminato)cadmium(II).

a quantum chemical analysis of spin systems in which one of the nuclei is unobservable in the given experiment and how information about the exchange process is gained using the effect of scalar spin–spin coupling on the spectral behavior of an observable nucleus coupled with the unobservable nucleus [12]. An unexpected result was obtained in the investigation of exchange processes in coordination compounds like complex I [8] (Fig. 7).

In spite of the rigid planar tricyclic structure of the molecule, the coalescence of the multiplets from the methine protons, –N=CH–, in its $^1$H NMR spectrum is similar to the same process observed for bis chelate II (Fig. 7) and differs from the latter only in that the transformations occur at higher temperatures. The realization of the degenerate ligand exchange mechanism $ML_2 + M^*L_2^* \leftrightarrow ML_2^* + M^*L_2$ in compounds like I is suggested by the examination of ICPs in the MUSEX 2D exchange spectra of for the mixture of the isotopomers $^{111}$Cd and $^{112}$Cd in the region of medium exchange rates.

The introduction of a methyl group into the diamine ring (passing to compound III) makes the signals from the protons of the six-membered chelate rings nonequivalent, owing to which the signals from the –N=CH– protons in the 1D spectrum are two doublets differing in chemical shifts, both characterized by a coupling constant of $^3J_{^{111}\text{Cd–N=CH–}} = 28$ Hz.

As the temperature is elevated, the components of either doublet broaden and coalesce almost synchronously. This is evidence that the life times of the two Cd–N bonds in the degenerate ligand exchange reaction are very similar. The presence of the methyl group $R^1$ in the diamine ring increases the activation barrier to ligand exchange by ≈8 kJ/mol over the barrier observed for the unsubstituted analogue.

The structure of dimer I presented in Fig. 7 is in agreement with X-ray crystallography data for *N*,*N*'-ethylenebis(thiosalicylaldiminato)cadmium(II) [13], which indicate that the central atom is pentacoordinated in the crystal. The Cd–L bond exchange leads to the formation of an intermediate dimer in which the coordination bonds around the Cd atom are arranged in the trigonal bipyramidal fashion. This structure is typical of structurally similar complexes of Zn(II) [14] and Cd(II) [15]. The series of concerted bond breaking and formation processes, which, according to the microscopic reversibility principle, includes intermediate polytopic rearrangements of the Berry pseudorotation type, ensures exchange of Cd atoms between the two different molecules of dimer I.

2D exchange spectroscopy data indicate that rapid intermolecular exchange reactions involving metal–ligand (M–L) bond breaking take place in solutions of planar cadmium complexes of type I (Fig. 7) with tetradentate ligands. A detailed analysis of the temperature-dependent changes in the peak shape for the signals from the –N=CH– protons in the 1D NMR spectrum and kinetic data (observation that the reaction is second-order) are fully consistent with the above inference.

### *Exchange Processes in Pb(II) Complexes*

The application of the MUSEX 2D exchange NMR technique to coupled spin systems made it possible to unambiguously identify the mechanisms of the structural nonrigidity of lead(II) bischelates and to distinguish two exchange processes, namely, degenerate intermolecular chemical ligand exchange and intermolecular spin exchange that is due to the fact that the anisotropy of the chemical shift of the heavy magnetic nucleus $^{207}$Pb makes a dominant contribution to the total longitudinal relaxation of the central atom [16].

The 1D dynamic NMR spectrum of bis(1-isopropyl-3-methylbenzylaldimino-5-selenopyrazolato)lead(II) (complex VII) enriched with $^{207}$Pb nuclei to the extent of 70% is shown in Fig. 8. At –40°C, the signal from the proton of the N=CH group is a superposition of the singlet signal from the Pb isotopomer ($S = 0$) and the doublet signal from the $^{207}$Pb isotopomer ($S = 1/2$, $^3J_{\text{Pb–H}} = 16.5$ Hz). As the temperature is elevated, all of the three signals broaden and coalesce, indicating the occurrence of metal–ligand bond breaking and formation reactions. The experimentally observed order of the reaction is 2, as is suggested by the linear dependence of the lifetimes of the spin states on the inverse total concentration of the complex in the solution. This is evidence of degenerate ligand exchange processes taking place. Theoretical simulation of the temperature-dependent line shape according to the ran-

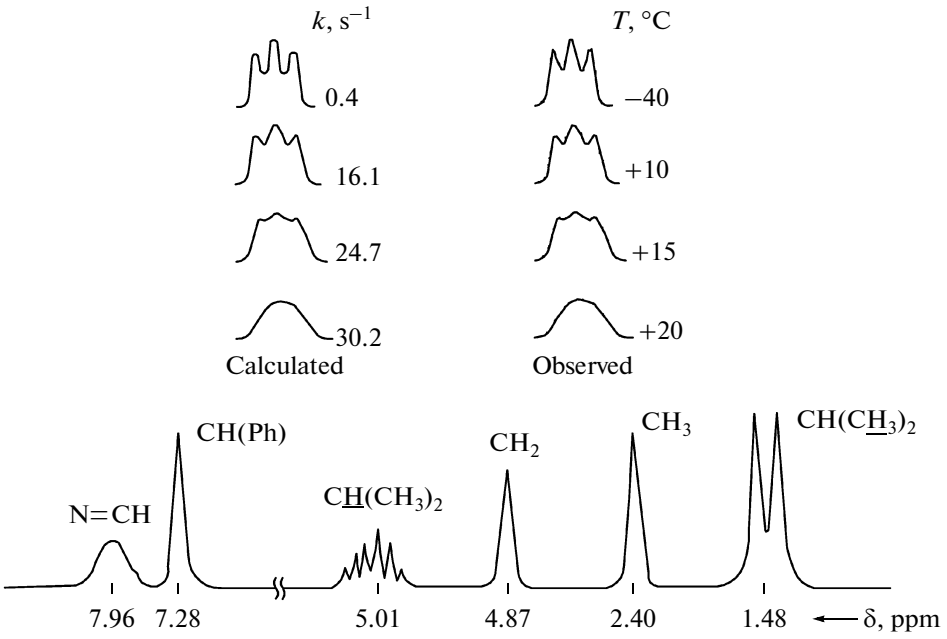


**Fig. 8.** $^{1}$H NMR spectra of complex VII (enriched with $^{207}$Pb to the extents of 70%) in tetrachloroethane and the evolution of the signal from the –N=CH– proton with temperature.

domization scheme is in agreement with the observed spectra (Fig. 8). It was assumed that the probability of ligand exchange between the isotopomeric complexes is proportional to their content.

The selective 2D exchange spectra of complex VII (Fig. 9a) recorded at 25 and 40°C show, in the region of the –N=CH– protons, three diagonal autopeaks from the Pb isotopomers ($S = 0$, central peak) and the $^{207}$Pb isotopomer ($S = 1/2$, extreme peaks) and six cross peaks of similar intensities. The two extreme cross peaks arise from ligand exchange processes between $^{207}$Pb isotopomer molecules; the four other ones, from ligand exchange between the $^{207}$Pb and Pb ($S = 0$) isotopomers. This kind of Fourier-transform 2D exchange NMR spectrum is strictly consistent with the exchange kinetics matrix of the intermolecular ligand exchange process.

Specific effects were discovered in the study of the low-temperature 1D $^{1}$H NMR spectra of complexes VII and VIII (Fig. 9b). Below 25°C, when the chemical exchange was slow, we observed a broadening of the spectral components of the doublet from the –N=CH– protons relative to the central signal. This broadening was concentration-independent and increased with a decreasing temperature.

At the same time, as the temperature was decreased from 0 to –50°C, the MUSEX 2D NMR spectra of compound VIII (Fig. 9a) retained the intradoublet pair of cross peaks, which were broadening together with the extreme autopeaks. These data indicate the occurrence of an intramolecular process that does not involve the nonmagnetic Pb(II) ($S = 0$) isotopomers and accelerates at the sample temperature is lowered. The presence of the "heavy nuclei" of lead in complex VIII made it possible to attribute the observed temperature-dependent dynamics of the MUSEX 2D exchange spectra to the rapid relaxation of the nuclei of the magnetic lead isotope via the chemical shift anisotropy mechanism [17]. This assumption was proved by the fact that the rate of the spin–lattice relaxation of the lead nuclei (recorded on spectrometers operating at 100, 200, and 500 MHz) increases with an increasing constant magnetic field $B_0$. The $T_1$ data obtained (96, 86, and 6 ms, respectively) are in good agreement with the theoretical linear $R_1^{SCA} = f(B_0^2)$ relationship [18]. This confirms that the above mechanism makes a dominant contribution to the total relaxation of the central metal atom.

## CONCLUSIONS

The 2D exchange NMR experiment with the multiplet-selective excitation of spin systems was used to unambiguously identify the mechanisms of the structural nonrigidity of bis chelate complexes of cadmium(II) and lead(II), including the topomerization of the coordination polyhedron and degenerate ligand exchange reactions with metal–ligand bond breaking via an associative mechanism. The latter process was discovered for the first time in planar tricyclic complexes of $^{111}$Cd(II) and $^{207}$Pb(II) with enaminothione (enaminoselenone) ligands.

Using VOF and the MUSEX technique, two exchange processes were distinguished in the lead complexes, namely, intermolecular degenerate chemical ligand exchange and intramolecular spin

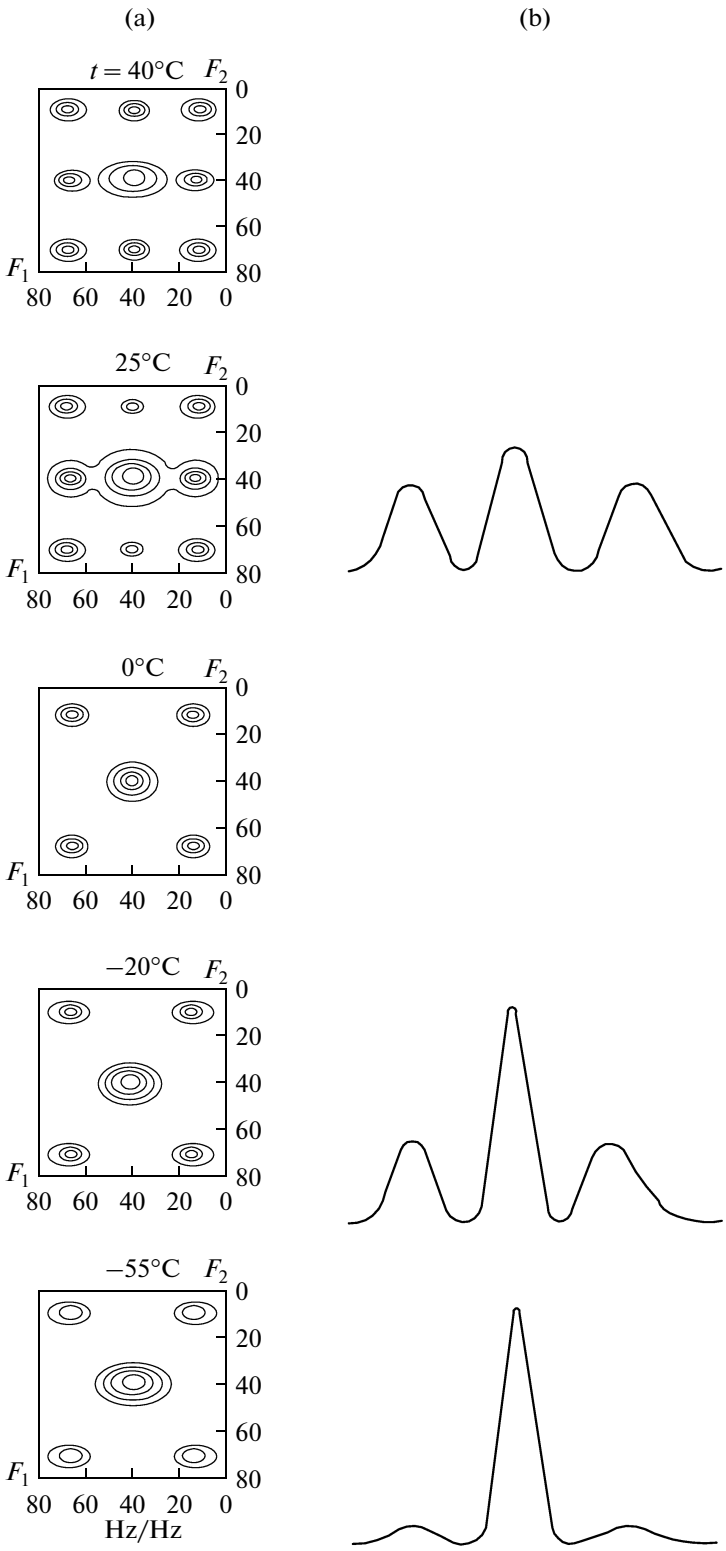


**Fig. 9.** $^{1}H$ NMR spectra of *N*,*N*'-ethylenebis(1-isopropyl-3-methyl-4-aldimino-5-selenopyrazolato)lead(II) (enriched with $^{207}Pb$ to the extent of 70%) in tetrachloroethane and the evolution of the signal from the –N=CH– proton with temperature: (a) temperature evolution of the MUSEX 2D exchange spectrum; (b) temperature evolution of the 1D NMR spectrum.

exchange due to the dominant contribution from the chemical shift anisotropy mechanism of relaxation of the heavy magnetic nucleus $^{207}$Pb to the total longitudinal relaxation of the central atom.

## ACKNOWLEDGMENTS

This study was carried out in the framework of the Project Part of the State Assignment in Science (project no. 4.967.2014/K).

## REFERENCES

1. R. Freeman, *Spin Choreography. Basic Steps in High Resolution NMR* (Oxford University Press, Oxford, 1998).
2. Yu. E. Chernysh, V. G. Vdovichenko, B. S. Luk'yanov, D. O. Kosarev, and V. S. Tsygankov, Russ. J. Phys. Chem. A **72**, 1542 (1998).
3. D. L. Turner, Prog. NMR. Spec. **17**, 281 (1985).
4. B. S. Wallace, *Pulsed Methods in 1D and 2D Liquid-Phase NMR* (Academic, New York, 1988).
5. Yu. E. Chernysh, G. S. Borodkin, and E. V. Sukholenko, J. Magn. Reson. **96**, 131 (1992).
6. Yu. E. Chernysh and V. A. Volynkin, Russ. J. Phys. Chem. B **7**, 371 (2013).
7. Yu. E. Chernysh, G. S. Borodkin, B. S. Luk'yanov, et al., *Selective NMR Fourier Spectroscopy and its Application to Study of Molecular Dynamics Processes* (Sev.-Kavk. Nath. Tsentr Vyssh. Shkola, Rostov-on-Don, 2002) [in Russian].
8. Yu. E. Chernysh, E. V. Sukholenko, and G. S. Borodkin, Appl. Magn. Reson. **4**, 69 (1993).
9. M. V. Potcalo, Yu. E. Chernysh, and D. V. Belov, in *Proceedings of the 7th International Workshop on Magnetic Resonance (Spectroscopy, Tomography, and Ecology)* (Inst. Fiz. Org. Khim, Yuzh. Univ., Rostov-na-Donu, 2006), p. 181.
10. R. Feynman, R. Leighton, and M. Sands, *The Feynman Lectures on Physics* (Addison Wesley, Reading, 1963), Vol. 3.
11. V. T. Panyushkin, V. D. Buikliskii, and S. N. Bolotin, *Application of of the Method of Spin Density Matrix in NMR and ESR Spectroscopy* (Prosveshchenie, Krasnodar, 1999) [in Russian].
12. R. Ernst, G. Bodenhausen, and A. Wokaun, *Principles of Nuclear Magnetic Resonance in One and Two Dimensions* (Clarendon, Oxford, 1987).
13. G. D. Fallon and B. U. Gatehouse, Acta Crystallogr. B **32**, 97 (1976).
14. M. Bonamico, G. Mazzone, and A. Vaciago, Acta Crystallogr. **19**, 898 (1965).
15. A. Domeniciano, L. Torelli, and A. Vaciago, J. Chem. Soc. A, No. 6, 1351 (1968).
16. Yu. E. Chernysh, G. S. Borodkin, M. S. Korobov, B. S. Luk'yanov, N. V. Stankevich, I. G. Borodkina, V. Yu. Vdovichenko, and Yu. M. Korobov, Russ. J. Coord. Chem. **28**, 170 (2002).
17. C. Stader and B. Wrackmeyer, J. Magn. Reson. **72**, 544 (1987).
18. W. P. Aue, E. Bartholdi, and R. R. Ernst, J. Chem. Phys. **64**, 2229 (1976).

*Translated by D. Zvukov*